

# TRIASSIC MONSOONAL CLIMATE AND ITS SIGNATURE IN LADINIAN-CARNIAN CARBONATE PLATFORMS (SOUTHERN ALPS, ITALY)

MARIA MUTTI AND HELMUT WEISSERT

*Geological Institute, Swiss Federal Institute of Technology, Sonneggstrasse 5, CH-8092 Zürich, Switzerland*

**ABSTRACT:** Paleoclimatic general circulation models suggest the existence of a monsoonal climate during the Permo-Triassic over wide parts of the megacontinent Pangea and its adjacent oceans. This paper discusses how Ladinian-Carnian sedimentary successions outcropping in the Southern Alps record the signature of this climate. Sedimentological associations of tepees capped by terra-rossa paleokarst, braided fluvial sediments capped by caliche soils, and evaporite beds alternating with clay-rich delta deposits all indicate that net precipitation values changed substantially over short geological time scales. Early diagenetic features including episodes of dissolution in stratigraphies of meteoric calcite cements, corrosion and hematization of siliciclastic detritus prior to deposition, early euhedral tectosilicate cementation, and dolomitization from evaporation-concentrated seawater record frequently changing paleohydrological conditions. Sedimentological and early diagenetic data recording highly variable, seemingly conflicting paleoclimate information can best be attributed to fluctuations in net precipitation intensities controlled by monsoonal climate, ranging from seasons to  $10^6$  yr.

$\delta^{18}\text{O}$  values in early meteoric cements ( $-5.2$  to  $-6.4\text{‰}$ ) reflect the presence of strongly depleted meteoric waters, which are not compatible with the Southern Alps paleolatitude or paleotopography in the Triassic and can be directly related to precipitation intensities associated with a monsoonal climate. Strong precipitation could have also resulted in decreased surface-water salinities and depleted  $\delta^{18}\text{O}$  in surface waters.  $\delta^{18}\text{O}$  time series from marine rocks and early meteoric cements indicate a trend from Middle Triassic values, generally depleted with respect to the expected marine signature, to less depleted Late Triassic values. This is interpreted to represent an unusually wet episode (high net precipitation), transitionally grading in the Late Triassic into a relatively arid period (or low net precipitation).

Despite the fact that several factors controlled the intensity of monsoonal precipitation, the effects of its variations through time are evident at different time scales in the Middle and Upper Triassic record of the Southern Alps.

## INTRODUCTION

The maximum continental aggregation in the Permian-Triassic formed the megacontinent Pangea and represented an exceptional phase in Earth's paleogeographic history (Wegener 1915; Valentine and Moores 1970; Ziegler et al. 1983). The role of land/ocean distribution in shaping ancient climates has long been recognized, and the effect of the Pangean configuration on global paleoclimate has been object of speculations for the past twenty years. The exposed land was divided symmetrically about the paleoequator between the Northern and Southern Hemispheres (Fig. 1A). These conditions were ideal for monsoonal circulation, as postulated by Robinson (1973), and later discussed qualitatively by Parrish et al. (1982) and Parrish (1993). Recent numerical paleoclimate experiments using Pangean geography also indicate a monsoonal climate (Crowley et al. 1989; Kutzbach and Gallimore 1989). The existence of the gigantic land mass of Pangea would have resulted in extreme continentality and a monsoonal circulation during the Triassic, with hot summers, cold winters, and large-scale summer and winter monsoon circulation (Kutzbach and Gallimore 1989). Climate models predict the maximum of seasonality in low and middle latitudes (Fig. 1B).

Sedimentary archives provide the possibility of testing the paleoclimate

simulations given for the Permian and the Triassic. So far only a few studies have focused on the question of how monsoonal climate left its specific signature in Permian or Triassic sediments. Dubiel et al. (1991) provided an example from the Colorado Plateau. They explained how sediments were formed under extremely variable climate conditions related to monsoonal climate. Triassic shallow marine carbonate strata exposed in spectacular successions in the Alps provide another archive to search for monsoon-related paleoclimate signatures. The sediments were deposited between about  $5^\circ$  to  $15^\circ$  paleolatitude in the eastern equatorial region of Pangea (Fig. 1A; Ziegler et al. 1983). The stratigraphic succession of mid to late Triassic sedimentary rocks reflects changing depositional environments ranging from carbonate platform to siliciclastic deltaic systems.

This paper examines in detail the sedimentary and diagenetic events recorded in Middle and Upper Triassic rocks outcropping in the Southern Alps, focusing on upper Ladinian/Carnian strata. Sedimentology, petrography, and isotope geochemistry are used to trace sedimentary and diagenetic history. Variations through time of sedimentary facies assemblages permit recognition of changing environmental conditions, which can be related to changes in net precipitation. Isotope geochemical data collected from carbonate cements and bulk sediments are used to follow long-term trends in diagenesis, paleohydrology, and precipitation history. We will show that paleoclimate fluctuations recorded in the rock record may be ascribable to monsoonal conditions operating at different temporal frequencies.

## THE PANGEAN MONSOON

The term "monsoon" means season in Arabic, but for climatologists it refers to a climate system in which most of the rainfall is during the summer. The most important feature of the monsoonal circulation is cross-equatorial flow, which results from the thermal and pressure contrast between the winter and summer hemispheres, and is driven mainly by sensible heat (Parrish 1993). The climatic consequences of monsoonal cross-equatorial flow are: (1) abundant but extremely seasonal rainfall, concentrated in the summer months, and (2) small annual temperature fluctuations in low latitudes (see Dubiel et al. 1991).

The Pangean continent was large and symmetrical with respect to the equator in the Triassic, with two halves flanking the equator (Parrish and Curtis 1982). The shape of Pangea enhanced the seasonally alternating circulation that would have occurred, due to thermal and pressure contrast, in both hemispheres. The interhemispheric thermal contrast would have been comparable to that now occurring during the summer Asian monsoon, but greater because both hemispheres were land (Crowley et al. 1989).

Kutzbach and Gallimore (1989) used several sensitivity experiments to study a range of possible climates associated with the Pangean configuration. Their results show features that correspond to the conceptual models. All experiments show strong monsoonal circulation, widespread year-round or seasonal aridity, summer monsoon precipitation along the southern and northern Tethyan coasts, and mid-latitude winter rain belts. In addition, they indicate extreme summer heat in the tropics, and a large seasonal range of temperatures for middle and high latitudes in continental interiors. They refer to this climate as to megamonsoonal.

We expect that such a megamonsoonal climate configuration would leave an indelible signature in the sedimentary record. Geochemical and

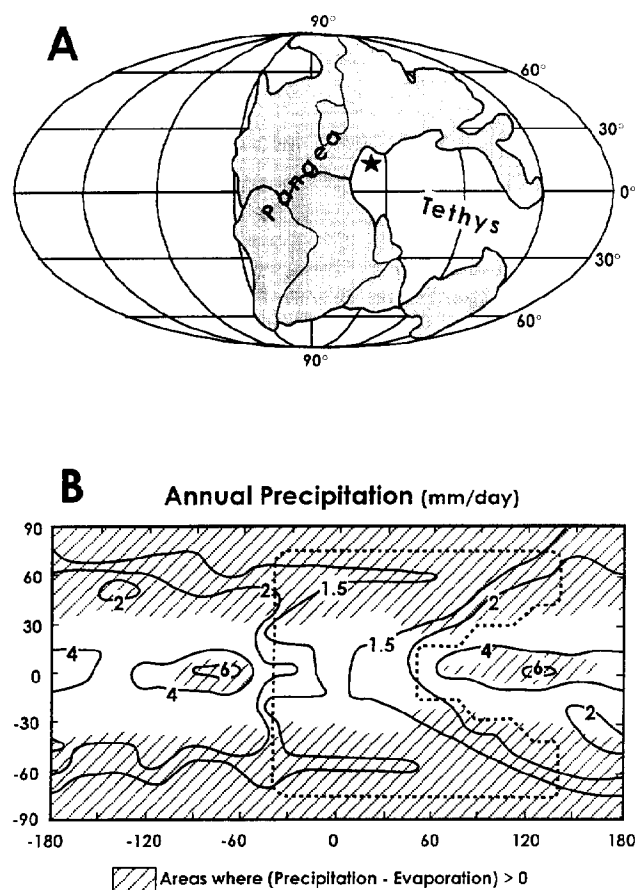


FIG. 1.—A) Schematic reconstruction of Pangea showing the approximate location of the Southern Alps (star). Modified from Dubiel et al. (1991). Paleogeography from Ziegler et al. (1983). B) Annual precipitation in millimeters/day, calculated using a low-resolution atmospheric general circulation model for a highly idealized geographic representation of Pangea (Kutzbach and Gallimore 1989). The idealized Pangea is marked by the stippled pattern. The hatched pattern indicates regions where precipitation exceeds evaporation. Experiments indicate a strong seasonality in low and middle latitudes, with seasonal intense precipitation and aridity. Modified from Kutzbach and Gallimore (1989).

sedimentological seasonality signals related to fluctuating moisture levels can be expected in carbonate and siliciclastic rocks. Regional facies comparisons should show that humidity in the equatorial regions of the east (western Tethys) was lower than in the west (e.g., Colorado Plateau; Dubiel et al. 1991). In addition, sedimentary records should reflect a reversal of equatorial flow during the maximum intensification of monsoonal circulation in the Late Triassic (Parrish and Peterson 1988). This would result in arid conditions in the eastern equatorial Pangea, contrasting with high rainfall along the western coast of Pangea. The coastlines flanking Tethys to the north and south should have been seasonally wet.

#### AREA OF STUDY AND STRATIGRAPHIC FRAMEWORK

Middle and Upper Triassic rocks crop out over a distance of 50 km in the Southern Alps (Fig. 2) in a complex system of folds and south-verging thrusts. Since the last century, the Triassic stratigraphic succession in the Lombardian Alps has been the object of many sedimentologic, stratigraphic, and biostratigraphic studies (e.g., Gnaccolini and Jadoul 1990, and cited references). Middle and Upper Triassic strata of the Lombardian Alps are characterized by carbonate sedimentation, interrupted in the mid-

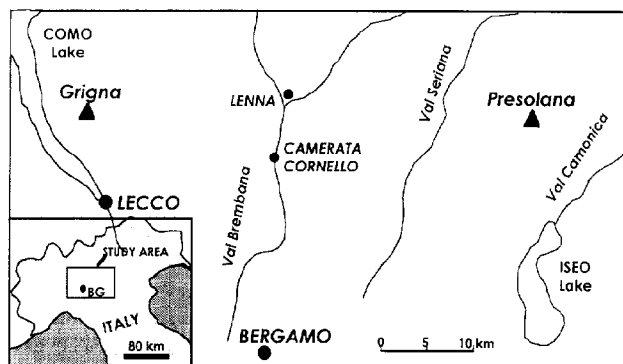


FIG. 2.—Simplified geological map of the Southern Alps.

Carnian by the deposition of the siliciclastic deltaic deposits of the Arenaria di Val Sabbia and San Giovanni Bianco, and in the early Rhaetian by the Riva di Soltò clays (Fig. 3). Because of the scarcity of age-diagnostic fossils, the accurate age of the platform units remains debatable. However, a combination of biostratigraphy and radiometric dating has allowed a precise correlation of Ladinian basinal units with the numerical time scales (Fig. 2; Brack and Rieber 1993). According to Brack and Rieber (1993) our Ladinian/Carnian sections span the time between 232 Ma and 223 Ma. An accurate description of the sedimentology of different Middle and Upper Triassic units has been given in detail in several papers (e.g., Garzanti and Jadoul 1985; Gnaccolini and Jadoul 1990; Mutti 1994), and only a brief summary is given here.

The Esino Limestone (late Anisian–Ladinian) developed as isolated carbonate banks associated with steep escarpments, facing small east-west-oriented basins. During the Ladinian, the basins were filled by carbonate debris and by volcanoclastics, as the Ladinian shallow water carbonate banks prograded into basinal settings and reached a thickness of 700–1000 m (Gaetani et al. 1986). In the late Ladinian, the Esino Limestone experienced prolonged subaerial exposure, when extensive karstic features developed on the former shelf and shelf margin, marking a temporal interruption of carbonate platform growth (Assereto et al. 1977; Mutti 1994).

Deposition of the Calcare Rosso (?late Ladinian–early Carnian) records a marine transgression over the karstified Esino Limestone (Assereto et al. 1977; Mutti 1994). The Calcare Rosso remains local in its geographic distribution, and its thickness varies between 0 and 50 m. For the present study, it turned out to be a valuable formation for preserving climate-diagnostic structures in peritidal cycles deformed into tepees and repeatedly capped by local paleokarstic horizons. In the early Carnian, extensive shallow-water sediments of the Breno Limestone and the Calcare Metallifero Bergamasco (early to mid Carnian) developed all over the Southern Alps and mark the reestablishment of shallow-water conditions over wide areas (Mutti 1992b). The Breno Limestone consists of 40–50 m of peritidal cycles with poorly deformed tepees and 60–70 m of submergence-dominated peritidal cycles; the Calcare Metallifero Bergamasco consists of 15–80 m of peritidal cycles (Mutti 1992c). A record of regional subaerial exposure at the top of the sequence marks the demise of the carbonate system.

In the mid-Carnian, terrigenous sediment input from the south, associated with a marked sea-level fall, led to the northward progradation of volcanoclastic deltaic complexes (Arenaria di Val Sabbia/AVS) and marly prodelta deposits (Gorno Formation) (Brusca et al. 1982; Garzanti 1985b). Carbonate sedimentation locally persisted in between areas of maximum sediment supply (Breno Limestone). Continental-evaporitic deposits of the San Giovanni Bianco Formation overlie deltaic sedimentary rocks of

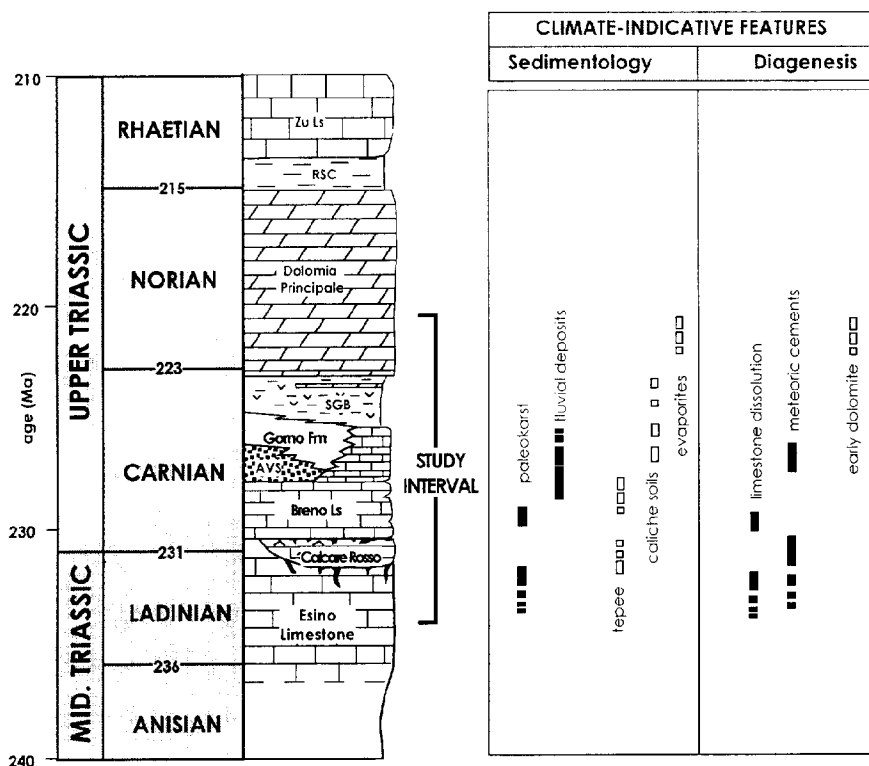


FIG. 3.—Middle and Upper Triassic stratigraphic units in the Southern Alps. AVS = Arenaria di Val Sabbia, SGB = San Giovanni Bianco, RSC = Riva di Solto Clays. To the right is sedimentologic and diagenetic evidence for climatic conditions in Middle and Upper Triassic. Open symbols refer to features that form under low net precipitation, filled symbols to features formed under high net precipitation. Ages are from Haq et al. (1987).

the Gorno Formation (see stratigraphic column, Fig. 3; Gnaccolini and Jadoul 1990).

Widespread carbonate sedimentation was regionally reestablished in the late Carnian, with the deposition across the Southern Alps of the cyclic peritidal sediments of the Dolomia Principale (Jadoul 1985). These deposits cover a relatively long time interval, ranging from the late Carnian into the late Norian. In the Rhaetian, carbonate sedimentation was interrupted when clays of the Riva di Solto Formation were deposited. Carbonate sedimentation gradually was reestablished in the mid Rhaetian, when shallow-water carbonates of the Zu Limestone were deposited.

#### THE LATE LADINIAN-LATE CARNIAN INTERVAL

In our search for paleoclimate signatures we focus on the upper Ladinian-Carnian sediments formed after the demise of the Esino carbonate platform and before the reestablishment of carbonate sedimentation of the Dolomia Principale at the end of the Carnian (Fig. 3). We will first discuss sedimentological and diagenetic features indicative of paleoclimatic conditions. In a second step, we will integrate stable-isotope data into the paleoenvironmental record.

#### SEDIMENTOLOGY

The purpose of this section is to focus on sedimentological features that form under specific climatic conditions and provide qualitative information on paleoclimate. Climate-indicative features fall into two major groups: indicators for high rainfall, such as karstic features and braided fluvial deposits, and for aridity, such as evaporites and desiccation cracks. The ratio between the relative abundance of the two groups in the investigated sections changes strongly throughout the sequence (Fig. 3), both in the long-term (formation scale;  $> 10^5$  yr) and the short-term scale (within the formations;  $1-10^5$  yr).

#### Evidence for High Rainfall

Karstic features are extensive in the Esino Limestone, the Calcare Rosso, and the Breno Limestone. They decrease upsection and are not present in Norian strata (Fig. 3). Dissolution cavities in the Esino Limestone extend down to a depth of 120 m from the platform top, within formerly submerged platform-margin facies. Fibrous, isopachous cements ("evinosponges", Frisia-Bruni et al. 1989) fill some of the dissolution cavities. In the Calcare Rosso the tepee-deformed peritidal strata are repeatedly capped by terra rossa karsts. Seasonality at the short-term scale is best documented by the association of tepee (desiccation cracks) and karstic features in the Calcare Rosso (Figs. 4, 5). The paragenesis of tepee facies of the Calcare Rosso record the alternation of dry conditions and the input of meteoric waters at temporal scales ranging from seasons to  $10^5$  yr. (Mutti 1994). At the top of the Breno Limestone (Metallifero), prolonged emergence of the platform resulted in erosion of part of the section and development of an extensive karstic network extending to a depth of 10–30 m (Mutti 1992b). Lead-zinc mineralization (fluorite, galena, and sphalerite) is associated with this exposure (Assereto et al. 1977) and is widespread in the Alpine area (Bechstädt 1975; Bechstädt and Dohler-Hirner 1983).

The presence of sediments deposited in braided river systems also provides indication for at least episodically high rainfall. The middle part of the Arenaria di Val Sabbia was deposited in fluviodeltaic environments under the influence of seasonal floods during the humid seasons (Gnaccolini 1983; Garzanti and Jadoul 1985). Many coarse clasts are intraformational and derived from erosion of muddy banks desiccated during dry seasons.

#### Evidence for Conditions of Low Rainfall and High Evaporation

The fluvial deposits of the Arenaria di Val Sabbia Formation are commonly interbedded with caliche and anhydrite nodules, indicating strong

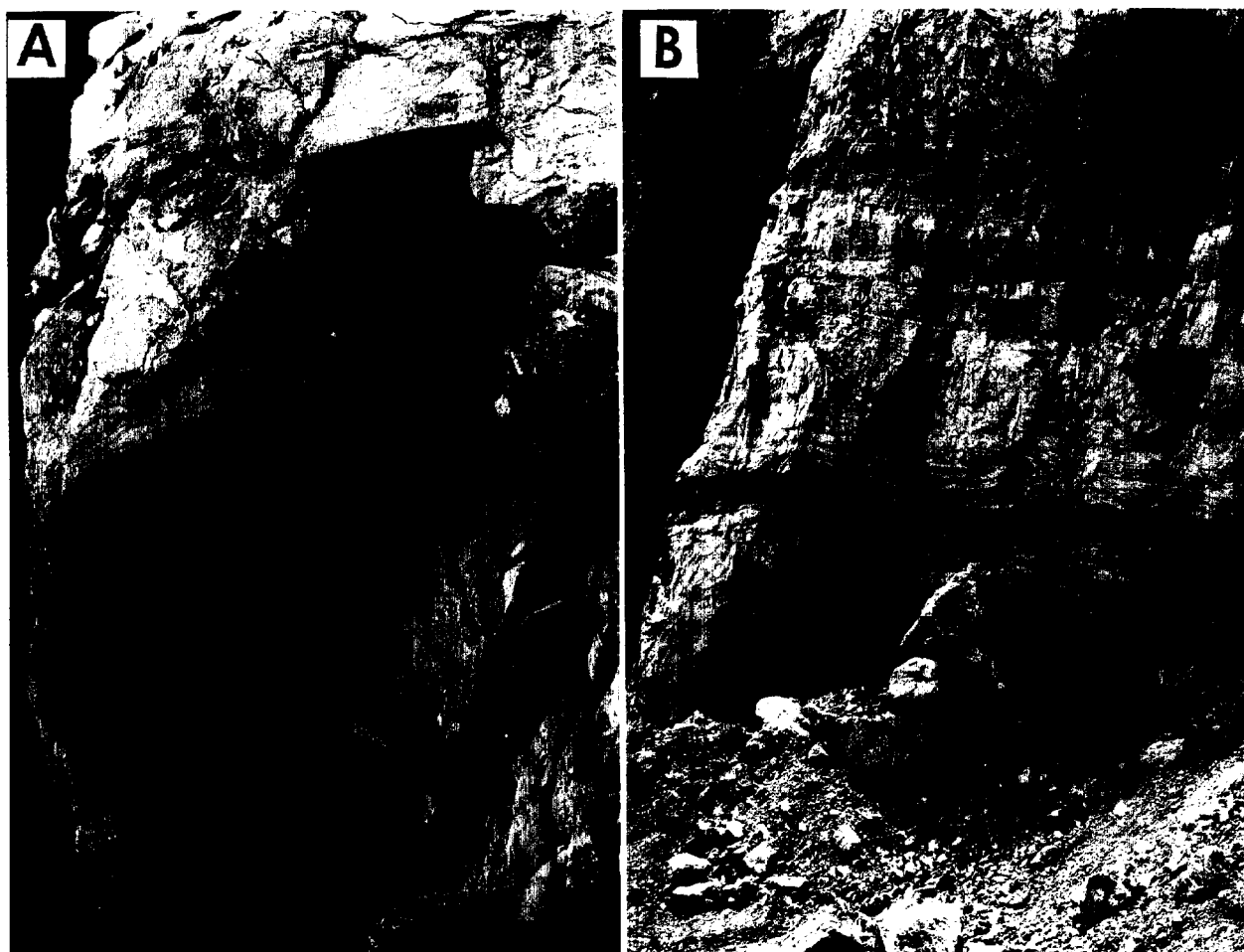


FIG. 4.—Climate-indicative sedimentological features. A) Terra-rossa paleokarst capping tepee-deformed peritidal strata (Calcare Rosso, Ladinian). B) Terra-rossa paleokarst capping a package of tepee-deformed peritidal strata. Tepees and karstic soils have traditionally been considered the product of processes related to subaerial exposure in arid and humid climates, respectively.

seasonal variations in net precipitation. Garzanti and Jadoul (1985) described caliche nodules reworked as intraclastic material by fluvial processes. When we trace the presence of evaporites as evidence for dry and warm climate conditions we find significant variability on the bedding scale and within the study interval. While no Ladinian evaporites have been reported, evaporites are of increasing abundance in the Southern Alpine sediments of mid-late Carnian and Norian age (Fig. 3). Evaporitic layers with enterolithic structures are present in the Arenaria di Val Sabbia (Garzanti 1985a); we interpret them as an indicator of low rainfall and high evaporation conditions. Evaporitic horizons are commonly intercalated with deltaic facies in the middle part and deltaic-fluvial sandstones with abundant caliche nodules dominate in the upper part (Garzanti and Jadoul 1985). Most widespread are evaporites in the upper Carnian sediments where anhydrite nodules are widespread in the alluvial deposits of the San Giovanni Bianco Formation. Low-precipitation and high-evaporation conditions predominate in the Dolomia Principale, where subaerial exposure of peritidal cycles at cycle tops is never associated with karst features, but rather with dolomitic caps and thick cement crusts, typical of arid vadose diagenesis (Hardie and Shinn 1986).

#### DIAGENESIS

Several studies have focused on the diagenesis of different stratigraphic units within the Ladinian and Carnian succession (Garzanti 1985a; Frisia-Bruni et al. 1989; Mutti 1992a, 1994). Here we discuss only diagenetic features that seem diagnostic of specific climatic conditions. In particular, we discuss the occurrence of extensive limestone dissolution and subsequent cement precipitation in meteoric environments of late Ladinian and early Carnian age. In addition, we review evidence for arid climate in the mid and late Carnian, based on studies of clay mineralogy made by Garzanti (1985a) and dolomitization by Frisia (1991).

#### *Dissolution and Early Cementation of Limestones*

Throughout the Ladinian and early Carnian record, there is extensive evidence of vadose and phreatic meteoric diagenesis in all the sections studied (Assereto et al. 1977; Frisia-Bruni et al. 1989; Mutti 1992a, 1994). Several karstic horizons, related to subaerial exposure events of different temporal hierarchies, are present throughout the sections (Fig. 3; see also



FIG. 5.—Paleokarsts in late Ladinian and early Carnian strata. In white carbonate clasts floating in a matrix of terra rossa. The borders of the clasts are marked by dissolution. A) Calcare di Esino (Late Ladinian); B) Calcare Rosso (Late Ladinian).

fig. 6 in Mutti 1994). Local subaerial exposure surfaces cap peritidal cycles, whereas major paleokarstic surfaces mark major interruptions in carbonate sedimentation (Mutti 1994). In association with both short- and long-term subaerial exposure, porosity was generated in the underlying strata. Limestones show extensive vuggy porosity, suggesting that large volumes of meteoric fluids, recharged from the subaerial exposure surfaces, were flowing through the strata. Micritic and fibrous pendant cements often line dissolution-enlarged pores, and document the occurrence of repeated phases of meteoric vadose diagenesis (Fig. 6).

Sparry calcite is present as a pore-filling cement in secondary pores and cavities. It is widespread throughout the Ladinian and lower Carnian strata. Optical and cathode-luminescence (CL) petrographic analyses allow recognition of three zones of low-Mg sparry calcite cements (Zones 1, 2, and 3; Fig. 7). Crosscutting relationships document that these zones precipitated in association with subaerial exposure during and immediately after deposition of the Calcare Rosso and Breno Limestone. Cement zones are bounded by dissolution events (Fig. 7D), and cements are postdated by precipitation of burial calcite cements and saddle dolomite (Mutti 1992a).

The petrographic and textural characteristics of the three zones of sparry calcite are listed in Figure 8. Cements show clear, equant crystals, and bright and nonluminescent banded CL patterns. These textural characteristics, together with the close paragenetic association with pendant ce-

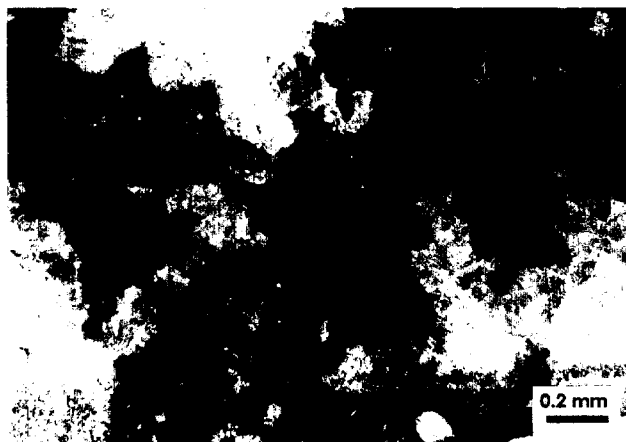


FIG. 6.—Climate-indicative diagenetic features. Photomicrograph shows dissolution features in the Calcare Rosso (Late Ladinian). Extensive formation of dissolution cavities is postdated by precipitation of pendant cements from cavity roof and deposition of microcrystalline silt on cavity floor (plane-polarized light).

ments and dissolution pores, suggest that the cements precipitated in a phreatic meteoric environment. The alternation in meteoric cement stratigraphies of dissolution and cementation suggests formation in a very dynamic system, with high recharge rates of meteoric waters and frequent oscillations in the calcite saturation state.

#### *Silicate Cements in Sandstones*

Garzanti (1985a, 1986) analyzed the petrography and diagenesis of the Arenaria di Val Sabbia, which consists of texturally immature lithic arenites, almost exclusively composed of volcanic rock fragments. Rock fragments, plagioclase, and quartz locally show evidence of corrosion and hematization prior to deposition (Fig. 3A), pointing to a climatic zonal distribution related to topography, with sporadic presence of deeply weathered, iron-rich soils in zones or periods of higher rainfall (Garzanti 1985a, 1986). Garzanti recognized the alternation of early diagenetic anoxic and oxic environments, with formation of pyrite and hematitic red beds. Pyrite is widespread in the mid-Carnian sediments, contrasting with the local presence of hematitic red beds in the middle Arenaria di Val Sabbia Formation and in the upper San Giovanni Bianco Formation. Iron for the pigments was derived from leaching of mafic silicates, beginning soon after deposition. In addition, multiple and euhedral tectosilicate cementation occurred as an early process predating compaction. Garzanti (1986) interpreted this to have occurred in an arid environment, favored by the episodic influx of silica-saturated alkaline waters in vadose and schizohaline conditions. This early diagenetic scenario supports frequently changing climatic conditions, with fluctuating intensities of net precipitation.

#### *Dolomitization*

Frisia (1994) and Frisia and Wenk (1993) recognized multistep dolomitization in the Dolomia Principale and characterized the different phases of dolomite with geochemical criteria. Oxygen isotope compositions range from +3‰ to -5‰, and according to Frisia (1991) the most enriched values are comparable with dolomite isotope signatures in modern sabkha dolomites, such as those analyzed by McKenzie (1981). These values have been modified during shallow burial. In particular, the stable-isotope composition and TEM characteristics suggest that the first, syndepositional phase of precipitation of dolomite occurred from evaporation-concen-

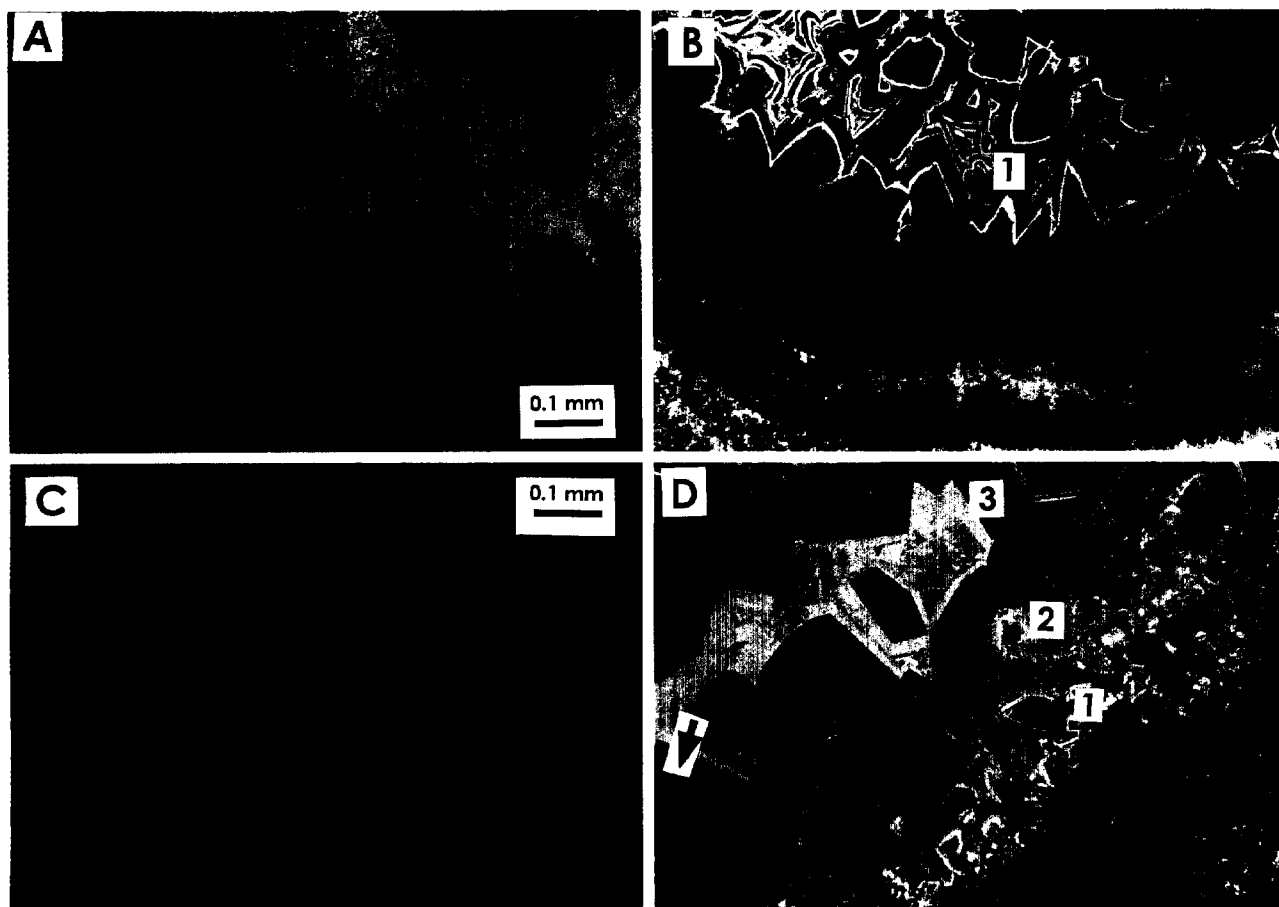


FIG. 7.—Meteoric cements and cathodoluminescence zones within upper Ladinian/lower Carnian strata. A, B) Plane-polarized light and cathodoluminescence paired images. An early fibrous cement is partially replaced by sparry calcite. Note the patchy luminescent pattern of the fibrous cement, and the clear, banded pattern of zone CL1. C, D) Plane-polarized light and cathodoluminescence paired images. Clear sparry calcite is present as pore-fill cement and contains several cathodoluminescence zones: CL1, CL2, and CL3. The three early zones are postdated by precipitation of a late cement, bright luminescent, which occurs as the last pore-filling phase. Note the dissolution contact between zone CL2 and CL3 (arrow).

trated seawater. The most important implication for our paleoclimate study is that the geochemistry of the early dolomites does not record the presence of any unaltered meteoric fluid percolating in the strata during or immediately following subaerial exposure, suggesting high aridity or low net precipitation values.

#### THE STABLE-ISOTOPE RECORD

##### Data

In our study of Triassic paleoclimate we combine stable-isotope data published in earlier studies (Frisia-Bruni et al. 1989; Mutti 1994) with new data on the stable-isotope composition of mid-Triassic sparry calcite cements. Stable-isotope analyses were performed according to the standard techniques using a VG Micromass-903 mass spectrometer at the laboratory for stable-isotope geochemistry at ETH-Zürich. The data are summarized in Figures 9 and 10. A list of the new samples analyzed is given in Table 1.

The bulk-rock isotopic composition of Triassic marine limestones and early fibrous cements is characterized by average  $\delta^{18}\text{O} = -5.8\text{‰} \pm 1.1\text{‰}$  and  $\delta^{13}\text{C} = 1.3\text{‰} \pm 0.6\text{‰}$  (Fig. 10). The sparry calcite cements measured for this study carry oxygen isotopic signatures centered around a value of  $\delta^{18}\text{O} = -6\text{‰}$  (Fig. 11). These values are in agreement with values pub-

lished in earlier studies. The carbon isotope composition of the sparry cements fluctuates between  $+0.5\text{‰}$  and  $+2\text{‰}$ . Zonation of sparry calcite cement is reflected in a trend to slightly more negative oxygen isotope values: Zone 1 =  $-5.2\text{‰}$ , Zone 2 =  $-5.9\text{‰}$ , and Zone 3 =  $-6.4\text{‰}$  (Fig. 10).

##### Discussion

All isotope data derived from marine components and early cements are depleted with respect to normal marine values. Scherer (1977) analyzed aragonite shells from Ladinian limestones in the Dolomites and calculated an oxygen and carbon isotope composition of  $\delta^{18}\text{O} = -2.3\text{‰}$  and  $\delta^{13}\text{C} = 3\text{‰}$  for Ladinian seawater. Mid-Triassic limestones and cements depleted in their oxygen isotope composition relative to Triassic seawater have also been reported by workers from age-equivalent strata in the northern Calcareous Alps (e.g., McKenzie and Lister 1983; Zeeh 1990). The depleted oxygen isotope compositions of limestones and cements have been interpreted either as indicators of meteoric or mixed marine-meteoric cementation (e.g., McKenzie and Lister 1983) or as signatures of deep burial diagenesis (e.g., Epting 1974; Frisia-Bruni et al. 1989).

Evidence for a meteoric origin of sparry calcite cements filling dissolution pores and cavities is given by the petrographic association with



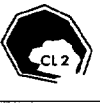
| Zones | Textures  | Zoning  | Color   | Boundaries   | $\delta^{18}\text{O}$ |
|-------|---|---|---|--|-----------------------|
| CL 1  | Circumgranular crystals, pore-lining and equant pore-filling, subhedral to anhedral crystals, 30–50 $\mu\text{m}$ wide.               |  | This zone is strongly banded following a circumgranular pattern and consist of non-luminescent bands with thin bright orange layers and evolves into mainly luminescent bands with non-luminescent bands.   | This cement overlies non-luminescent early fibrous cements with a dissolution boundary.                  | -5.2                  |
| CL 2  | Circumgranular crystals as pore-lining and equant crystals as pore-filling, subhedral to anhedral crystals, 50–70 $\mu\text{m}$ wide. |  | This zone is characterized by a relatively homogeneous dark orange color, with thin bright orange bands towards the margins of the crystals. The presence of inclusions imparts a slightly patchy luminescence color at the nucleus of some crystals. | It grows in optical continuity over zone 1. A well marked dissolution event occurs at the end of zone 2. | -5.9                  |
| CL 3  | Crystals are equant, both pore-lining and pore-filling, 100–250 $\mu\text{m}$ wide.   |  | This zone is non-luminescent with few thin bright orange bands.   | This zone is separated from zone 2 by a dissolution event  | -6.4                  |

FIG. 8.—Characteristics of the three zones: Zones CL 1, CL 2, and CL 3 recognized in the meteoric cements.

vadose cements and paleokarst surfaces and by the isotope geochemical signature (Fig. 10). Clear CL patterns of sparry calcite cements (Fig. 8) suggest that the cements retained their original geochemical composition and were not affected by isotope reequilibration during deep burial.

If we interpret the oxygen isotope signature of sparry calcite cements as the result of early calcite precipitation from meteoric waters, then we are confronted with two unknowns, the temperature of precipitation and the isotopic composition of meteoric waters. The composition of meteoric waters in modern low-latitude areas is generally similar to the composition of the seawater (Yurtsever and Gat 1981). To obtain the values we have measured in the rock, with a value of  $\delta^{18}\text{O}_w$  around 0 to  $-2\text{‰}$ , precipitation should occur at relatively high temperatures (up to  $40^\circ\text{C}$ ) (Fig. 12A), a value that seems unrealistic for shallow groundwater. If the temperature of precipitation was lower ( $< 20\text{--}25^\circ\text{C}$ ), then the cements were precipitated from increasingly depleted meteoric waters, with a  $\delta^{18}\text{O}_w$  reaching values near  $-6\text{‰}$ . This value is too negative for the average low-latitude ( $5\text{--}15^\circ\text{N}$ ) meteoric cements precipitated from waters whose composition is

controlled only by a latitude effect. If we choose this second scenario, we must assume that mid-Triassic meteoric waters were depleted relative to average low-latitude waters, and were influenced by either an altitude effect, a continentality effect, or an amount effect (Rozanski et al. 1992).

On the basis of paleogeographic reconstructions, we can exclude any important altitude or continentality effect influencing the composition of Triassic rainwater in the Western Tethys. However, monsoonal climate predicted by climate models would result in strong and episodic rainfall in equatorial areas (Fig. 1B). As a consequence, we should expect strong isotopic depletion in meteoric waters, such as is observed in modern tropical and monsoonal locations. Rozanski et al. (1992) were able to show how in present-day monsoonal regions the amount effect has a predominant effect on the isotopic composition of the rainfall. The oxygen isotopic composition of the rainfall is inversely proportional to the amount of precipitation (Fig. 12B).

Episodic strong precipitation could even have had an impact on the isotopic composition of mid-Triassic oceanic surface waters. This is observed today in areas of episodic rainfall such as the Tarawa Atoll in the Western Pacific, where coral-skeletal carbonate precipitated from seawater carries the signature of rainfall variability over the last 100 years. The

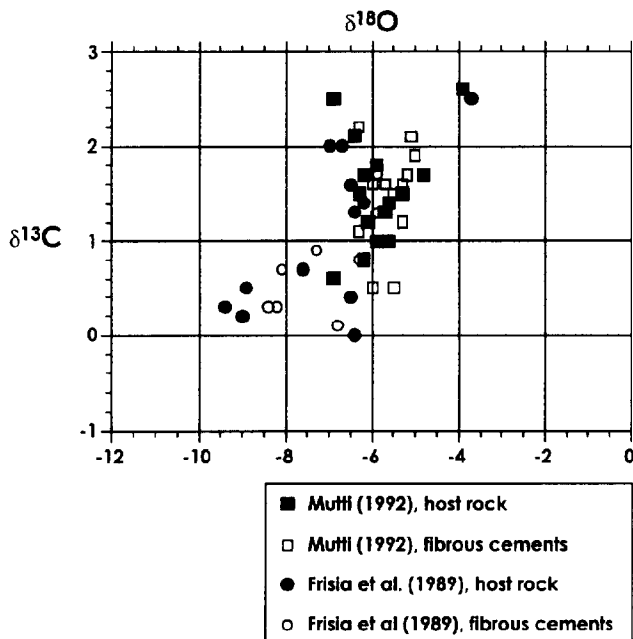


FIG. 9.—Stable-isotope data for Ladinian and early Carnian host rock.

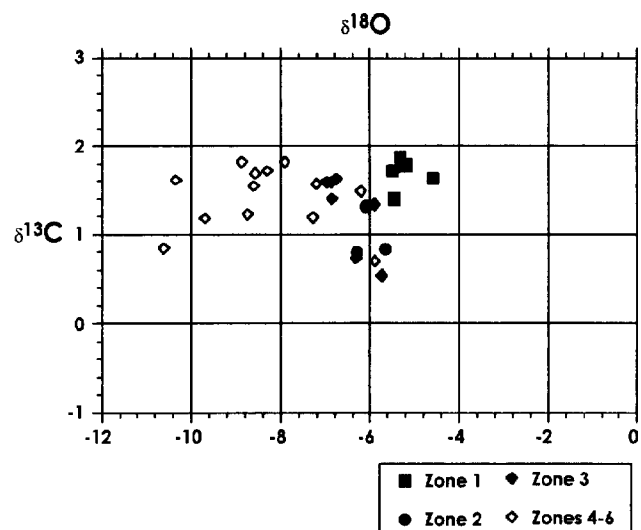


FIG. 10.—Stable-isotope data for meteoric cements.

TABLE 1.—List of the stable-isotope composition of sparry meteoric to burial calcite samples measured in Middle Triassic strata

| Sample      | CL Zone | $\delta^{13}\text{C}$ | $\delta^{18}\text{O}$ |
|-------------|---------|-----------------------|-----------------------|
| J 3-2C      | CL 1    | 1.9                   | -5.3                  |
| J 3-3C      | CL 1    | 1.7                   | -5.5                  |
| J 3-4C      | CL 1    | 1.6                   | -4.6                  |
| M 2-4C      | CL 1    | 1.4                   | -5.5                  |
| J 3-8C      | CL 1    | 1.8                   | -5.2                  |
| M 9-3       | CL 2    | 1.3                   | -6.1                  |
| J 3-1C      | CL 2    | 0.8                   | -5.7                  |
| J 3-5C      | CL 2    | 0.8                   | -6.3                  |
| M 19-1      | CL 3    | 1.6                   | -6.9                  |
| M 19-3      | CL 3    | 1.6                   | -6.7                  |
| J 8-1C      | CL 3    | 1.6                   | -7.0                  |
| M 72-1-2C   | CL 3    | 0.7                   | -6.3                  |
| M 69-2-2C   | CL 3    | 1.3                   | -5.9                  |
| M 72-1-3C   | CL 3    | 1.4                   | -6.8                  |
| J 8-1C      | CL 3    | 0.5                   | -5.7                  |
| M 19-2      | CL 4-6  | 1.8                   | -7.9                  |
| M 9-2       | CL 4-6  | 1.6                   | -10.3                 |
| M 19-4      | CL 4-6  | 1.5                   | -6.2                  |
| M 9-4       | CL 4-6  | 1.7                   | -8.3                  |
| M 19-3      | CL 4-6  | 1.6                   | -7.2                  |
| M 19-5      | CL 4-6  | 1.8                   | -8.9                  |
| M 8-6C      | CL 4-6  | 0.8                   | -10.6                 |
| M 69-1-1-3C | CL 4-6  | 1.7                   | -8.6                  |
| M 72-1-1C   | CL 4-6  | 1.2                   | -7.3                  |
| M 69-2-1C   | CL 4-6  | 0.7                   | -5.9                  |
| M 69-1-2C   | CL 4-6  | 1.5                   | -8.6                  |
| M 19-1C     | CL 4-6  | 1.2                   | -8.7                  |
| M 19-2C     | CL 4-6  | 1.2                   | -9.7                  |

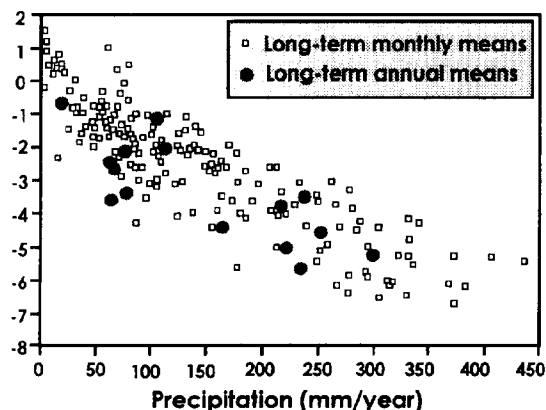
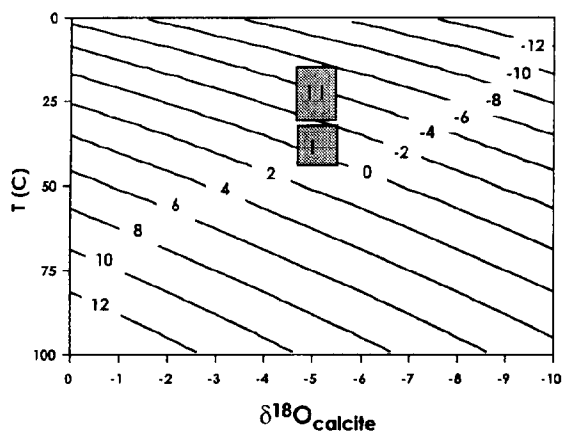


FIG. 11.—A) Temperature/oxygen plot for Ladinian/Carnian values. The graph is based on the equation of Epstein et al. (1951). B) Long-term monthly and annual mean  $\delta^{18}\text{O}$  values for tropical island stations of the IAEA/WMO global network ( $20^{\circ}\text{S}$  to  $20^{\circ}\text{N}$ ), plotted as a function of mean monthly precipitation. The depletion in  $\delta^{18}\text{O}$  is directly proportional to the amount of precipitation: this is known as the amount effect. Modified from Rozanski et al. (1992).

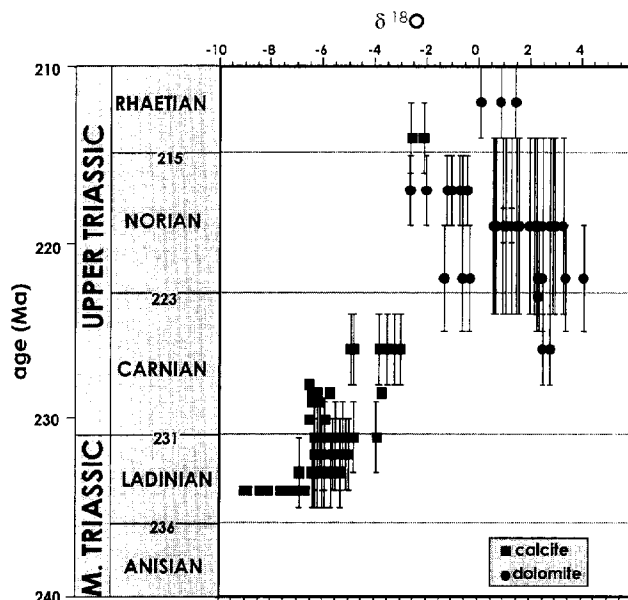


FIG. 12.—Long-term  $\delta^{18}\text{O}$  trends based on over 150 data points compiled from Scherer (1977), McKenzie and Lister (1983), Taylor (1983), Frank (1986), Frisia-Bruni et al. (1989), Zeeh (1990), Frisia (1991), and Mutti (1992a). Bars indicate uncertainty in age determination. Calcite and dolomitic samples are plotted separately.

variability of oxygen reaches up to 1‰, and the associated salinity change varies from 35 to 31‰ (Dunbar and Cole 1993).

The isotopic composition of mid-Triassic marine carbonates could therefore also reflect decreased surface water salinities and depleted oxygen isotope values in surface waters, as a consequence of increased precipitation under monsoonal conditions. The amount effect has so far not been considered as a possible variable affecting Triassic carbonate isotopic signatures. However, judging from available paleoclimate information, its impact on the isotope values may have been considerable.

Deep burial diagenesis resulted in partial overprint of Triassic climate signatures. Evidence for deep burial is given by microfractures, affecting host rocks and early cement generations, filled by late calcite cements. The samples affected by microfracturing containing the late calcite cements show remarkably depleted isotopic compositions of  $-9\text{‰}$  to  $-12\text{‰}$  (Frisia-Bruni et al. 1989). The precipitation of late burial calcite cements is accompanied by saddle dolomite formation, a further indicator of deep burial diagenesis (Mutti 1992a). The values reported for the investigated sections for host rock and cements are consistently less depleted with respect to these extreme burial values, and they correspond to the values interpreted by Frisia-Bruni et al. (1989) as diagenetically stabilized low-magnesium calcite (dLMC).

#### LONG-TERM ISOTOPIC TRENDS

In order to understand the significance of late Ladinian and Carnian data within a longer-term time series, we made a compilation of all available data on the isotopic composition of Middle and Upper Triassic rocks. We plotted the composition of marine host rock and of early meteoric cements with respect to age (Fig. 12). We have systematically selected the least depleted values, to rule out the effect of burial diagenesis and to have a record as close as possible of the primary marine values. Both calcitic and dolomitic samples have been selected. Dolomite values have been later converted into calcite, assuming a fractionation factor  $\epsilon = 3.8\text{‰}$  (Fig. 13; McKenzie 1981).



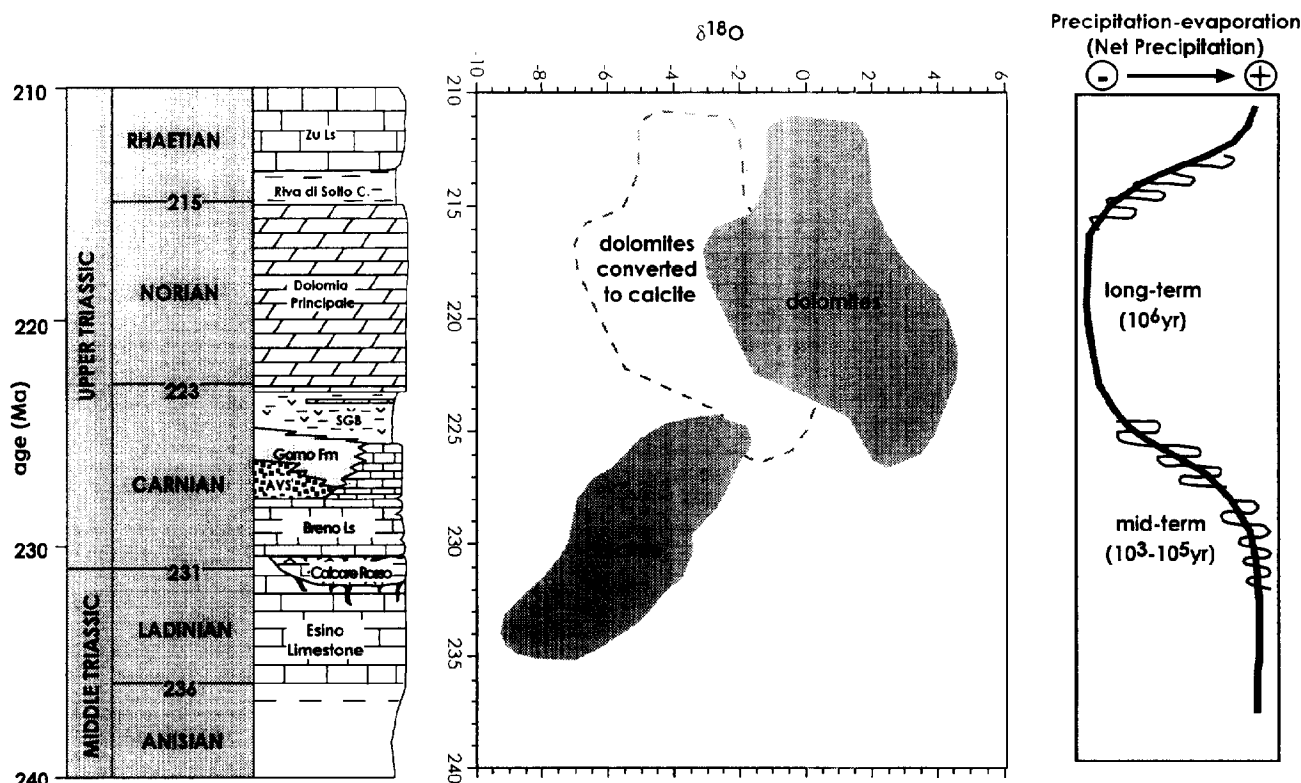


FIG. 13.—Synthetic field of Middle and Upper Triassic isotopic data paired with the corresponding stratigraphic units. Dolomitic samples have been converted to calcite, assuming a fractionation factor  $\epsilon$  of 3.8. The curve to the right shows long-term changes ( $10^6$  yr) in monsoon intensities, as interpreted from the  $\delta^{18}\text{O}$  values. Shorter-term changes ( $10^3$ – $10^5$  yr), deduced from the sedimentological and early diagenetic record, are schematically shown superimposed on the long-term trend.

A general trend emerges from the available data set (Fig. 13): marine rocks and early cements of Ladinian–early Carnian age are generally depleted in  $\delta^{18}\text{O}$  with respect to the normal marine values. In addition,  $\delta^{18}\text{O}$  composition in bulk samples and cements become systematically less depleted from the Ladinian to the Norian. This trend is reversed in the Rhaetian, when  $\delta^{18}\text{O}$  compositions again become depleted.

The long-term isotope trend we recognize in the Southern Alpine sedimentary rocks can be compared with similar trends recorded in Permo-Triassic alluvial sediments from North America and India. Dutta and Suttner (1986), in a study on alluvial sandstones recognized a trend from more to less negative  $\delta^{18}\text{O}$  values in diagenetic clays, ranging in age from the Permian to the late Triassic. They interpreted it as an indicator of changing paleolatitude and therefore changing freshwater isotope compositions. The data from the Southern Alps, a low-latitude environment, suggest that oxygen isotope signals in the Permo-Triassic could fluctuate also because of changes in precipitation rates and rainfall intensity.

#### CLIMATE CYCLICITY, MONSOONS, AND THE TRIASSIC RECORD

The middle Triassic carbonate-siliciclastic formations cropping out in the Southern Alps preserve sedimentological and geochemical signatures indicative of paleoclimatic conditions (Fig. 13). Evidence of contrasting humid-warm and dry-warm climate occurs throughout the Middle Triassic at varying time frequency scales.

(1) Rainfall history resulting in limestone dissolution and subsequent cementation of dissolution cavities in carbonate strata can be deciphered from carbonate cement stratigraphies. Associated sedimentological features such as tepees suggest that episodes of intense rainfall and high water tables alternated with times of aridity and evaporative conditions on the

mid-Triassic carbonate platforms. Co-occurrence of indicators of dry and of humid climate within individual beds suggests high-frequency fluctuations in climate on the order of years to  $10^5$  yr.

(2) The sedimentology of fluvial sediments again shows remarkable fluctuations in the hydrologic budget of the Middle Triassic Tethyan region. Braided-river deposits are linked with caliche horizons and point to strongly fluctuating precipitation rates during the time of formation of the Middle Triassic Arenarie di Val Sabbia. Climate fluctuated between dry and humid conditions again with frequencies of years to  $10^5$  yr.

(3) The Middle and Upper Triassic sequence studied preserves not only traces of seasonality or episodic rainfall and aridity but also a record of long-term climate fluctuation between dominantly dry times (carbonate buildups) and humid episodes (braided-river deposits). These fluctuations occurred with frequencies of  $10^4$  to  $10^6$  yr.

(4) An additional tracer of paleoclimate can be seen in the oxygen isotope signature of calcite cements and potentially of bulk carbonate. Middle Triassic oxygen isotopic compositions that are interpreted to be of early diagenetic origin seemed in equilibrium with isotopically depleted meteoric waters. A long-term trend to isotopically less depleted calcite cements can be recognized if we trace the sequences into the Late Triassic, when widespread dolomitization affected carbonates throughout the southern Alpine depositional realm.

In agreement with model predictions, the described paleoclimate indicators suggest seasonality of climate and fluctuations in rainfall intensity at different frequencies ranging between a seasonal scale and  $10^6$  yr scale. On the basis of the described sedimentological and isotope geochemical data, a monsoonal climate may best explain the observations. The fluctuations in net precipitation and monsoonal intensity at frequencies of thousands to hundreds of thousand years call for a mechanism that could

affect the monsoonal intensity. A number of factors, varying at time scales ranging from  $10^3$  to  $10^6$  yr, control the intensity of the modern Indian monsoon and the sedimentary record of the Western Arabian Sea (Prell and Kutzbach 1992). Orbital components are an additional important forcing factor affecting the monsoonal climate and its preservation in the sedimentary record. The temporal scales of seasonal climatic variations recorded by sedimentologic and diagenetic events in Middle Triassic rocks are of comparable magnitude.

The Middle Triassic represents an unusually wet episode (or high net precipitation), transitionally grading in the Late Triassic into a relatively arid period (or low net precipitation). The relatively arid conditions that existed during the Late Triassic in the eastern coast of Pangea (Southern Alps), documented in this paper, contrast with the high-rainfall conditions recorded by Dubiel et al (1991) from the west coast of Pangea. Parrish and Peterson (1988) identified major changes of Late Triassic wind directions as recorded in eolian sediments. They suggested that monsoonal circulation became strong enough during the Late Triassic to influence circulation on the western side of Pangea and draw moisture along the equator from the west. Our result is in agreement with their hypothesis.

### CONCLUSIONS

(1) Paleoclimate models allow a deductive approach to Earth and climate history. Sedimentary successions allow testing of paleoclimate simulations based on general circulation models. The Triassic of the Alps is an example of how seemingly conflicting paleoclimate information can be interpreted with a monsoonal climate that was dominant during the Permian-Triassic over wide parts of Pangea and its adjacent oceans.

(2) The described stratigraphic, sedimentologic, and petrographic data indicate a strong seasonality in the Ladinian-Carnian section of the Southern Alpine test area. This change in climatic conditions is observed at different temporal scales, ranging from seasons to  $10^6$  yr. These changes are in agreement with a monsoonal circulation model, and can be related to different degrees of intensity of the monsoons.

(3) This study suggests not only that the  $\delta^{18}\text{O}$  of meteoric waters was controlled by temperature and the latitude effect, but also that in times of episodic high precipitation a considerable amount effect may have altered the isotopic signal of rainwater and sea-surface water.

(4) Meteoric cements may provide a very promising tool in tracing the variations in precipitation intensities through time and help to constrain paleoclimate models.

### ACKNOWLEDGMENTS

We acknowledge the support from the Stable Isotope Laboratory at ETH (Judy McKenzie and Stefano Bernasconi). Karl Föllmi and Stefano Bernasconi (both ETH Zürich) read an early draft of the paper and provided useful comments and discussions. Diki Garzanti (Milano) shared unpublished results. Urs Gerber printed all the photographs. Kurt Grimm and Judith Parrish provided very competent and careful reviews. The project was in part supported by the Swiss National Science Foundation.

### REFERENCES

- ASSERETO, R.L.A.M., JADOU, F., AND ONENETTO, P., 1977, Stratigrafia e metallogenesi del settore occidentale del distretto a Pb, Zn, fluorite e barite di Gorno (Alpi Bergamasche): Rivista Italiana di Paleontologia e Stratigrafia, v. 83, p. 395-532.
- BECHTOLD, T., 1975, Lead-zinc ores dependent on cyclic sedimentation (Wetterstein limestone of Bleiberg-Kreuth, Carinthia, Austria): Mineralium Deposita (Berlin), v. 10, p. 234-248.
- BECHTOLD, T., AND DOLHER-HIRNER, B., 1983, Lead-zinc deposits of Bleiberg-Kreuth, in Scholte, P.A., Bebout, D.G., and Moore, C.M., eds., Carbonate Depositional Environments: American Association of Petroleum Geologists Memoir 33, p. 55-63.
- BRACK, P., AND RIEBER, H., 1993, Towards a better definition of the Anisian/Ladinian boundary: New biostratigraphic data and correlations of boundary sections from the Southern Alps: Eclogae Geologicae Helveticae, v. 86, p. 415-527.
- BRUSCA, C., GAETANI, M., JADOU, F., AND VIEL, G., 1982, Paleogeografia ladinico-carnica e metallogenese del Sudalpin: Società Geologica Italiana, Memorie, v. 22, p. 65-82.
- CROWLEY, T.J., HYDE, W.T., AND SHORT, D.A., 1989, Seasonal cycle variations on the supercontinent of Pangea: implications for Early Permian vertebrate extinctions: Geology, v. 17, p. 457-460.
- DUBIEL, R.F., PARRISH, J.T., PARRISH, J.M., AND GOOD, S.C., 1991, The Pangean megamonsoon—Evidence from the Upper Triassic Chinle Formation, Colorado Plateau: PALAIOS, v. 6, p. 347-360.
- DUNBAR, R.B., AND COLE, J.E., 1993, Coral Records of Ocean-Atmosphere Variability: National Oceanic and Atmospheric Administration, Climate and Global Change Program, Special Report 10.
- DUTTA, P.K., AND SUTTNER, L.J., 1986, Alluvial sandstone composition and paleoclimate, II. Authigenic mineralogy: Journal of Sedimentary Petrology, v. 56, p. 346-358.
- EPTING, M., 1974, Ablagerung, Diagenese und Paleogeographie der mitteltriadischen Sedimente in der Ostalpbaiern, Italien [unpublished Ph.D. thesis]: University of Münster, Germany, 254 p.
- EISEN, S., BUCHSBAUM, R., LOWENSTAM, H., AND UREY, H.C., 1951, Carbonate-water isotopic temperature scale: Geological Society of America Bulletin, v. 62, p. 417-426.
- FRANK, S.M., 1986, Die Raibl-Gruppe und ihr liegendes im Oberostalpin Graubündens: die Entwicklung einer evaporitischen Karbonatplattform unter wechselnden Klimabedingungen [unpublished Ph.D. thesis]: Zürich, Eidgenössische Technische Hochschule, 240 p.
- FRISIA, S., 1991, Caratteristiche sedimentologiche ed evoluzione diagenetica della Dolomia Principale (Norico) del Lago d'Idro e delle Dolomiti di Brenta [unpublished Ph.D. thesis]: University of Milano, Milano, Italy, 156 p.
- FRISIA, S., 1994, Mechanisms of complete dolomitization in a carbonate shelf: comparison between the Norian Dolomia Principale (Italy) and the Holocene of Abu Dhabi Sabkha, in Purser, B., Tucker, M., and Zenger, D., eds., Dolomites: A Volume in Honour of Dolomieu: International Association of Sedimentologists Special Publication 21, p. 55-74.
- FRISIA, S., AND WENK, R.H., 1993, TEM and AEM study of pervasive, multi-step dolomitization of the Upper Triassic Dolomia Principale (Northern Italy): Journal of Sedimentary Petrology, v. 63, p. 1049-1058.
- FRISIA-BRUNI, S., JADOU, F., AND WEISSERT, H., 1989, Evaporites in the Triassic Esino Limestone (Southern Alps): documentation of early diagenetic lithification and late diagenetic overprint: Sedimentology, v. 36, p. 685-699.
- GAETANI, M., GINAOTTI, R., JADOU, F., CIARAPICA, G., CIRILLI, S., LUALDI, A., PASSERI, L., PELLEGRINI, M., AND TANNOIA, G., 1986, Carbonifero Superiore, Permiano e Triassico dell'area Lariana: Società Geologica Italiana, Memorie, v. 32, p. 5-48.
- GARZANTI, E., 1985a, Petrography and diagenesis of Upper Triassic volcanic arenites (S. Giovanni Bianco, Gorno and Val Sabbia Formations; Bergamasche Alps): Società Geologica Italiana, Bollettino, v. 104, p. 3-20.
- GARZANTI, E., 1985b, The sandstone memory of the evolution of a Triassic volcanic arc in the Southern Alps, Italy: Sedimentology, v. 32, p. 423-433.
- GARZANTI, E., 1986, Source rock versus sedimentary control on the mineralogy of deltaic volcanic arenites (Upper Triassic, Northern Italy): Journal of Sedimentary Petrology, v. 56, p. 267-275.
- GARZANTI, E., AND JADOU, F., 1985, Stratigrafia e paleogeografia del Carnico Lombardo (Sondaggio S. Gallo, Valle Brembana): Rivista Italiana di Paleontologia e Stratigrafia, v. 91, p. 295-320.
- GNACCOLINI, M., 1983, Un apparato deltizio Triassico nelle Prealpi Bergamasche: Rivista Italiana di Paleontologia e Stratigrafia, v. 88, p. 599-612.
- GNACCOLINI, M., AND JADOU, F., 1990, Carbonate platform, lagoon and delta "high-frequency" cycles from the Carnian of Lombardy (Southern Alps, Italy): Sedimentary Geology, v. 67, p. 143-159.
- HARDIE, L.A., AND SHINN, E.A., 1986, Carbonate depositional environments, modern and ancient: 3, Tidal Flats: Colorado School of Mines Quarterly, v. 81, 74 p.
- HAQ, B.U., HARDENBOL, J., AND VAIL, P.R., 1987, Chronology of fluctuating sea levels since the Triassic: Science, v. 235, p. 1156-1166.
- JADOU, F., 1985, Stratigrafia e paleogeografia del Norico superiore delle Prealpi Bergamasche occidentali: Rivista Italiana di Paleontologia e Stratigrafia, v. 91, p. 479-512.
- KUTZBACH, J.E., AND GALLIMORE, R.G., 1989, Pangean climates: Megamonsoons of the megacontinent: Journal of Geophysical Research, v. 94, p. 3341-3357.
- McKENZIE, J.A., 1981, Holocene dolomitization of calcium carbonate sediments from the coastal sabkhas of Abu Dhabi, U.A.E.: a stable isotope study: Journal of Geology, v. 89, p. 185-198.
- McKENZIE, J.A., AND LISTER, G.S., 1983, Origin of alternating calcite and dolomite void-filling cements ("Grossolites") in middle Triassic reefs of the Northern Limestone Alps near Innsbruck, Austria: 4th International Association of Sedimentologists Regional Meeting, Split, Yugoslavia, p. 109-110.
- MUTTI, M., 1992a, Caratterizzazione sedimentologica e diagenetica di superfici di discontinuità al tetto della piattaforma ladinica lombarda [unpublished Ph.D. thesis]: University of Milano, Milano, Italy, 219 p.
- MUTTI, M., 1992b, Facies a tepee del Calcare Rosso (Ladinico superiore, Alpi Lombarde): meccanismi di formazione ed implicazioni per la stratigrafia del Ladinico-Carnico Lombardo: Giornale di Geologia, v. 54, p. 147-162.
- MUTTI, M., 1992c, Cycle stacking patterns in Ladinian/Carnian carbonate platforms: implications for recognition of regional sequences in the Lombardic Alps, in Sequence Stratigraphy of European Basins: CNRS-IPF (Centre National de la Recherche Scientifique-Institut Français du Pétrole), Dijon, France, p. 154-155.
- MUTTI, M., 1994, Association of tepees and paleokarst in the Ladinian Calcare Rosso (Southern Alps, Italy): Sedimentology, v. 40, p. 621-641.
- PARRISH, J.T., 1993, Climate of the Supercontinent Pangea: Journal of Geology, v. 101, p. 215-233.
- PARRISH, J.T., AND PETERSON, F., 1988, Wind directions predicted from global circulation models and wind directions determined from aeolian sandstones of the western United States—a comparison: Sedimentary Geology, v. 56, p. 261-282.

- PARRISH, J.T., AND CURTIS, R.L., 1982, Atmospheric circulation, upwelling, and organic-rich rocks in the Mesozoic and Cenozoic Eras: Palaeogeography, Palaeoclimatology, Palaeoecology, v. 40, p. 261-282.
- PARRISH, J.T., ZIEGLER, A.M., AND SCOTSE, C.R., 1982, Rainfall patterns and the distribution of coals and evaporites in the Mesozoic and Cenozoic: Palaeogeography, Palaeoclimatology, Palaeoecology, v. 40, p. 67-101.
- PRELL, W.L., AND KUTZBACH, J.E., 1992, Sensitivity of the Indian monsoon to forcing parameters and implications for its evolution: *Nature*, v. 360, p. 647-652.
- ROBINSON, P.L., 1973, Paleoclimatology and continental drift, in Tarling D.H., and Runcorn, S.K., eds., *Implications of Continental Drift to the Earth Sciences*, I: London, Academic Press, p. 449-476.
- ROZANSKI, K., ARAGUAS-ARAGUAS L., AND GONFIANTINI, R., 1992, Isotopic patterns in modern global precipitation, in Swart, P.K., et al., *Climate Change in the Continental Isotopic Record: American Geophysical Union Monograph 78*, p. 1-36.
- SCHERER, M., 1977, Preservation, alteration and multiple cementation of aragonite skeletons from the Cassian beds (Southern Alps), petrographical and geochemical evidence: *Neues Jahrbuch für Geologie und Paläontologie, Abhandlungen*, v. 154, p. 3213-262.
- TAYLOR, S., 1983, A stable isotope study of the Mercia Mudstones (Keuper Marl) and associated sulphate horizons in the English Midlands: *Sedimentology*, v. 30, p. 11-31.
- VALENTINE, J.W., AND MOORES, E.M., 1970, Plate-tectonic regulation of faunal diversity: *Nature*, v. 228, p. 657-659.
- WEGENER, A., 1915, *Die Entstehung der Kontinente und Ozeane*: Druck und Verlag von Friedr. Vieweg und Sohn, Braunschweig, 94 p.
- YURTSEVER, Y., AND GAT, J.R., 1981, Atmospheric waters, in Gat, J.R., and Gonfiantini, R., eds., *Stable Isotope Hydrology, Deuterium and Oxygen-18 in the Water Cycle*: Vienna, Austria, International Atomic Energy Agency, Technical Report 210, p. 193-142.
- ZEEH, S., 1990, Fazies und Diagenese des obersten Wettersteinkalkes der Gailtaler Alpen (Drauzug, Oesterreich): *Freiburger Geowissenschaftliches Beiträge*, v. 1, 210 p.
- ZIEGLER, A.M., SCOTSE, C.R., AND BARRETT, S.F., 1983, Mesozoic And Cenozoic paleogeographic maps, in Broesche, P., and Sündermann, J., eds., *Tidal Friction and The Earth's Rotation II*: Berlin, Springer-Verlag, p. 240-252.

Received 26 September 1994; accepted 17 January 1995.